Compact Dense Wavelength-Division (De)multiplexer Utilizing a Bidirectional Arrayed-Waveguide Grating Integrated With a Mach–Zehnder Interferometer

Sitao Chen, Xin Fu, Jian Wang, Yaocheng Shi, Sailing He, *Fellow, IEEE, Fellow, OSA*, and Daoxin Dai, *Member, IEEE*

***Abstract*—A compact wavelength-division (de)multiplexer is proposed and demonstrated experimentally to achieve doubled channel number and halved channel spacing by utilizing a bidirectional arrayed-waveguide grating integrated with an Mach–Zehnder interferometer optical interleaver. As an example, an 18-channel wavelength-division (de)multiplexer with a channel spacing of 200 GHz is designed and fabricated. The measured excess loss is about 8 dB and the channel crosstalk is $-15 \sim -18$ dB. The footprint of this fabricated (de)multiplexer is about 520 μm $\times$ 190 μm.**

***Index Terms*—Arrayed-waveguide grating (AWG), bi-directional, interleaver, silicon nanowire.**

I. Introduction

DENSE wavelength-division-multiplexing (DWDM) has been used very successfully as one of the most important techniques to improve the capacity of an optical communication link. It is well known that a wavelength division (de)multiplexer is a key component [1], which can be realized with micro-ring resonators (MRRs) [2]–[6], etched-diffraction gratings (EDGs) [7], [8], as well as arrayed-waveguide gratings (AWGs) [9]–[22]. MRR is a simple element to achieve passive and active devices for many applications [23]–[25]. Particularly, an array of MRRs cascaded in series can be used to realize a multi-channel (de)multiplexer with an ultra-small footprint while it is not easy to have uniform channel spacing due to the fabrication deviation. Both AWGs and EDGs are planar waveguide (de)multiplexers, which enable multiple channels in parallel with very uniform channel spacing and thus have been widely used in practical WDM systems. A general issue for an EDG is that high quality grating-facets are needed critically to minimize the excess loss, and an EDG usually has lower dispersion ability than an AWG due to the small interference order. Therefore, an AWG is usually preferred for DWDM applications. Furthermore, it is easy to realize $N \times N$ AWG, which is useful for some applications. Therefore, in the past decades AWGs have attracted intensive attention and been realized on various material platforms, like silica-on-silicon [9], InP [10], polymer [11], Si_3N_4 [12], [13], and silicon-on-insulator (SOI) [14]–[22]. Among them, the sub-micron optical waveguides based on SOI enable ultra-sharp bending due to the very high index contrast and provide one of the most promising platforms to realize ultra-small AWGs [14]–[22].

In the past decade, SOI-nanowire AWGs have been developed by several groups. For the AWGs with relatively large channel spacing (e.g., 400 GHz), the footprint is small and the performances are pretty good [16]–[19]. However, for those SOI-nanowire AWGs with smaller channel spacing (e.g., $50 \sim 200$ GHz), which are desired for DWDM applications, the device footprint increases greatly and the performance (e.g., the channel crosstalk) degrades significantly [16], [20], [21]. For example, the channel crosstalk of the SOI-nanowire AWG (de)multiplexers demonstrated in [16] are $-17 \sim -23$ dB, $-15 \sim -20$ dB, and $-9 \sim -15$ dB, respectively, when with the channel spacing is 400, 250, and 100. It is a challenge to realize an ultra-small wavelength division multiplexer with a dense channel spacing as well as excellent performances.

Note that an optical interleaver can be used to divide the input 2*N* channels ($\lambda_1, \lambda_2, \ldots, \lambda_N, \ldots, \lambda_{2N}$) into an odd group ($\lambda_1, \lambda_3, \ldots, \lambda_{2N-1}$) and an even group ($\lambda_2, \lambda_4, \ldots, \lambda_{2N}$) so that these two groups with doubled channel spacing can be separately (de)multiplexed by using e.g., *N*-channel AWG (de)multiplexers with doubled channel-spacing. Usually two AWG (de)multiplexers are needed to work with an optical interleaver (as shown in Fig. 1). In [26], a Mach–Zehnder interferometer (MZI) and two AWGs have been monolithically integrated on silica-based PLC platform to realize a (de)multiplexer with 64 channels and a channel spacing of 25 GHz. One should note that such a configuration including an optical interleaver and two AWG (de)multiplexers is pretty complicated and the footprint is very large. Furthermore, it is not easy to realize two AWG (de)multiplexers with critically aligned central wavelengths for all the channels because there are some fabrication deviations, especially for devices on SOI platform. This might be the reason

Manuscript received January 8, 2015; revised February 8, 2015 and February 17, 2015; accepted February 17, 2015. Date of publication March 15, 2015; date of current version March 20, 2015. This work was supported in part by a 863 project under Grant 2011AA010301, the Nature Science Foundation of China under Grants 6141101056, 91233208, and 61422510, the Doctoral Fund of Ministry of Education of China under Grant 20120101110094, and the Fundamental Research Funds for the Central Universities.

The authors are with the Centre for Optical and Electromagnetic Research, State Key Laboratory for Modern Optical Instrumentation, Zhejiang Provincial Key Laboratory for Sensing Technologies, Zhejiang University, Hangzhou 310058, China (e-mail: dxdai@zju.edu.cn).

Color versions of one or more of the figures in this paper are available online at http://ieeexplore.ieee.org.

Digital Object Identifier 10.1109/JLT.2015.2405510

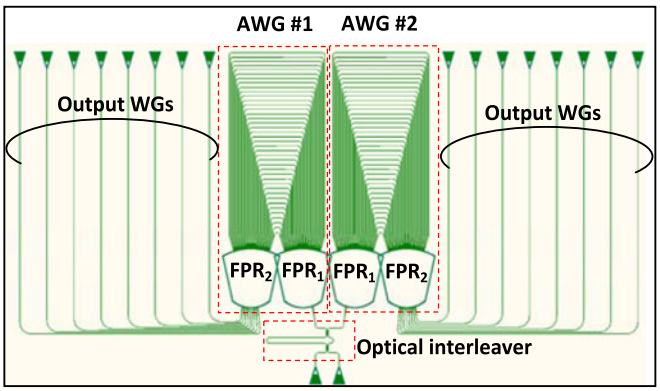

Fig. 1. Schematic configuration of a traditional dense wavelength division multiplexer consisting of two AWGs and an MZI-based optical interleaver.

that there is no much work reported for the realization of such a monolithically integrated device on SOI nanowires.

In this paper, we demonstrate a dense wavelength division (de)multiplexer by integrating an MZI-based optical interleaver with only one $(N+1)\times(N+1)$ AWG (de)multiplexer, which has doubled channel spacing of that for the multiplexed input signal. And this $(N+1)\times(N+1)$ AWG works bi-directionally so that it plays the role of two $1\times N$ AWGs whose central wavelengths for all the channels are aligned perfectly. In [27] and [28], a bi-directional AWG structure was utilized to eliminate the polarization dependent wavelength shift when working with a polarization diversity circuit. One should also realize that there are some drawbacks for a bi-directional AWG, like the degradation of the return loss and the directivity due to the light loopback. Furthermore, the insertion loss also increases a little because the input waveguide is positioned at the edge. Fortunately, the performance degradation is acceptable and excellent bi-directional AWGs have been demonstrated [27], [28]. In this paper, the demonstrated dense wavelength division (de)multiplexer consisting of a bi-directional AWG and an MZI-based optical interleaver also shows excellent performances while the channel spacing is halved and the channel number is doubled.

II. Structure and Design

Fig. 2 shows the schematic configuration of the present wavelength division de-multiplexer consisting of a bi-directional AWG and an optical interleaver based on an asymmetrical MZI. As shown in Fig. 2, the bi-directional AWG has $N+1$ access optical waveguides at both sides. Among the access optical waveguides at each side, there is an input waveguide and N output waveguides. In the present case, the access waveguide at the inner-edge works as the input waveguide in order to have a convenient layout design (avoiding any crossings). There are two input waveguides for the bi-directional AWG to be connected respectively with the two output ports of the MZI interleaver in the front. This MZI is designed to have a free spectral range (FSR) equal to the channel spacing of the bi-directional $(N+1)\times(N+1)$ AWG. As a consequence, the wavelength-division-multiplexed signals $(\lambda_1, \lambda_2, \ldots, \lambda_{2N})$ with a channel spacing of $\Delta\lambda_{\rm ch}$ launched from one of the input ports of the

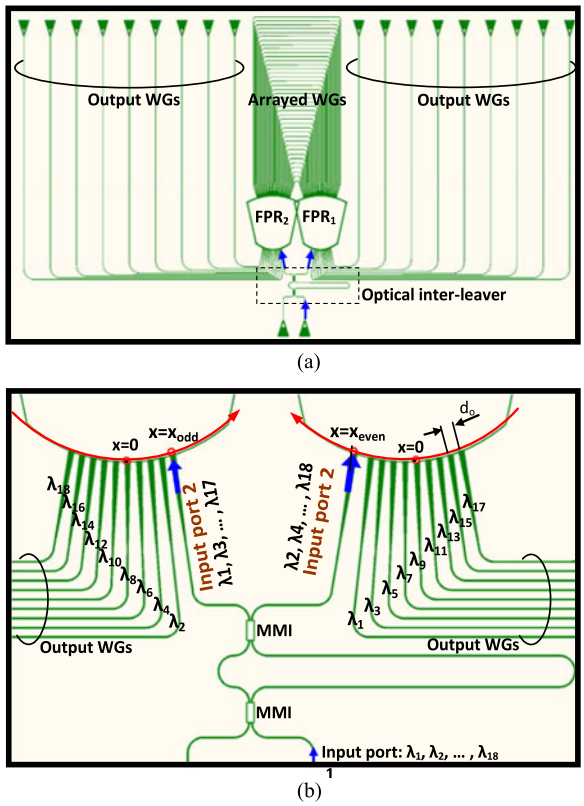

Fig. 2. (a) Schematic configuration of the present dense wavelength division multiplexer consisting of a bi-directional AWG and an MZI-based optical interleaver. (b) The enlarged view for the MZI-based optical interleaver connecting with the two input waveguides of the bi-directional AWG.

MZI are then interleaved into two groups, i.e., the odd group $(\lambda_1, \lambda_3, \ldots, \lambda_{2N-1})$ and the even group $(\lambda_2, \lambda_4, \ldots, \lambda_{2N})$. The channel spacing for these two groups of channels becomes doubled, i.e., $\Delta\lambda'_{\rm ch} = 2\Delta\lambda_{\rm ch}$. Since these two groups of channels share the same waveguide grating and the free propagation regions (FPRs), it is expected that the separation d_o between the adjacent output waveguides at both sides are the same. As shown in Fig. 2(b), the output waveguides are arranged uniformly with a separation d_o, which is given by

$$d_o = D\Delta\lambda_{\rm ch} = \frac{R_a}{d_a}\frac{\Delta L\lambda_c}{c}\frac{n_g}{n_{\rm FPR}}\Delta\lambda_{\rm ch} \tag{1}$$

in which λ_c is the central wavelength, ΔL is the length difference between the adjacent arrayed waveguides, n_g is group index of the arrayed-waveguide mode, $n_{\rm FPR}$ is the slab mode index in FPRs, $\Delta\lambda_{\rm ch}$ is the desired channel spacing, R_a is the length of the FPR region, d_a is the separation between the adjacent arrayed waveguides at the end connecting with the FPRs. In the present design, the output waveguides at both sides are arranged symmetrically to make the layout design convenient. The two groups of signals are then injected to the two input waveguides of the bi-directional AWG respectively. Since the central wavelengths for the two groups of channels are interleaved, the two input waveguides of the bi-directional AWG should be positioned asymmetrically. For the odd group of channels $(\lambda_1, \lambda_3, \ldots, \lambda_{2N-1})$, the position of the input waveguide is given by $x_{\rm odd} = d_o$ INT(N/2), where INT(x) is the function to achieve

the maximal integer less than x. Correspondingly the position of the input waveguide for the even group of channels ($\lambda_2, \lambda_4, \ldots, \lambda_{2N}$) is given by $x_{\rm even} = x_{\rm odd} + d_o/2$.

As example, a 220 nm-thick SOI wafer is considered and the designed SOI nanowire is 460 nm wide and 220 nm high to be singlemode for the arrayed waveguides. In this case, the values of the following parameters for the central wavelength $\lambda_c = 1555.75$ nm are given as: $n_{\rm FPR} = 2.84769$, and $n_g = 4.1$. The channel spacing of the bi-directional AWG is chosen to be $\Delta\lambda'_{\rm ch} = 3.2$ nm ($\Delta f'_{\rm ch} = 400$ GHz), and the channel number is $N = 9$ so that a 18-channel dense de-multiplexer with a channel spacing of $\Delta\lambda_{\rm ch} = 1.6$ nm ($\Delta f_{\rm ch} = 200$ GHz) will be enabled. The other parameters of the bi-directional AWG are given as follows. The diffraction order is chosen as $m = 30$ to make the FSR be larger than the product $N_{\rm ch}\Delta\lambda_{\rm ch}(=28.8\,{\rm nm})$ so that 18 channels are available. The path difference between the adjacent arrayed waveguides is $\Delta L = 19.64$ μm, calculated with the formula $\Delta L = m\lambda_c/n_{\rm eff}$, where λ_c is the central wavelength ($\lambda_c = 1555.75$ nm), and $n_{\rm eff}$ is the effective index of the transversal electric (TE) fundamental mode in the arrayed waveguide ($n_{\rm eff} = 2.37734$). When choosing the gap between the adjacent arrayed waveguides at the end connecting with the FPRs, one should make a tradeoff carefully. In order to reduce the excess loss and the facet reflection, a small gap is desired. However, a small gap will introduce the lag effect in the dry etching process [29], [30]. This usually makes the part with small gaps in the arrayed waveguides non-uniform, which introduces some notable phase errors and thus some channel crosstalk. In order to make the etching uniformly regarding the lag effect, in our design we choose the gap width as $w_{\rm gap} = 300$ nm [31]. The separation between the adjacent arrayed waveguides at the end connecting with the FPRs is chosen as $d_a = 1.6$ μm. The length of the FPRs is $R_a = 100$ μm, and correspondingly the end separation between the output waveguides is about $d_o = 3.69$ μm and. With this design, the footprint for the part including the arrayed waveguides and the two FPRs is about 440 μm $\times$ 190 μm.

For the design of the MZI-based optical interleaver, the length difference $\Delta L_{\rm MZI}$ of the MZI's arms should be chosen to achieve an FSR $\Delta\lambda_{\rm FSR\_MZI}$ matched to the channel spacing of the bi-directional AWG, i.e., $\Delta\lambda_{\rm FSR\_MZI} = \Delta\lambda'_{\rm ch} = 3.2\,{\rm nm}$. In addition, the central wavelengths of the MZI and the AWG should be also aligned well. As a result, the length difference is chosen as $\Delta L_{\rm MZI} = 189.5$ μm optimally. For the 3 dB power splitter/combiner in the MZI optical interleaver, we use 2 $\times$ 2 multimode-interference (MMI) couplers to be fabrication tolerant. The pair-interference mechanism in a MMI section is utilized and the input/output waveguides are positioned at $x = \pm w_{\rm MMI}/6$. Regarding that the separation of the input/output waveguides should be large enough to avoid any undesired coupling, we choose the width of the MMI section as $W_{\rm MMI} = 2.4$ μm. The length of the MMI coupler is optimized by maximizing the transmission at the crossing port of a symmetric MZI structure consisting of a pair of 2 $\times$ 2 MMI couplers, as shown by the insets in Fig. 3(a). According to the MZI's principle, the transmission at the crossing port is given by $|\kappa t|^2$ because the constructive interference happens (where κ and t are the cross and through coupling ratio). A three-dimensional finite-difference time-domain method is used for the simulation of light propagation in the symmetric MZI and the simulation result for the optimal design with $L_{\rm MMI} = 6.3$ μm is shown by the blue curve in Fig. 3(a). It can be seen that the theoretical transmission at the crossing port of the MZI is about 85% ($\sim$0.7 dB) over a broad band ranging from 1.5 to 1.6 μm, which indicates that the designed MMI coupler enables a low-loss MZI-based optical interleaver in theory. Here very weak oscillation is observed and this is from the F-P cavity effect due to the reflection at the facets of these two MMIs. For an MZI, the extinction of the cross port is high intrinsically in theory while the extinction of the through port is dependent of the power splitting ratio of the MMI-based 3 dB couplers. Here the wavelength dependence of the power splitting ratio of the present 3 dB MMI coupler is also calculated, as shown in Fig. 3(b). It can be seen that the power splitting ratio of the MMI-based 3 dB couplers is wavelength dependent in some degree. This is the reason why the extinction of the transmission at the through port of the MZI is wavelength dependent (as shown in Fig. 7 below).

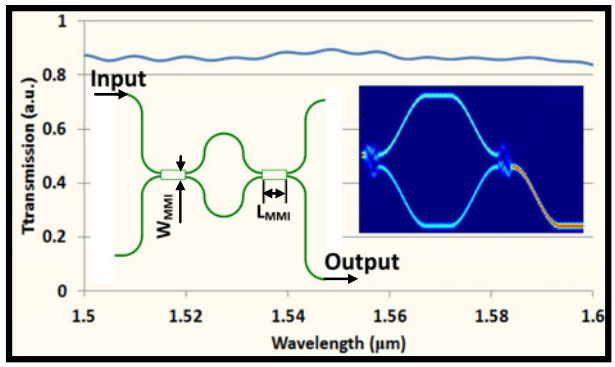

(a)

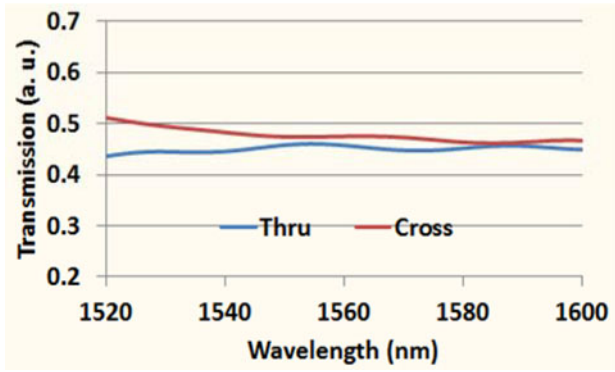

(b)

Fig. 3. (a) Simulated transmission of an MZI consisting of the MMI couplers with $W_{\rm MMI} = 2.4$ μm and $L_{\rm MMI} = 6.3$ μm. The inset shows the propagation for the optimized structure. (b) The simulated wavelength dependence for the power splitting ratio of the MMI coupler.

III. Fabrication and Characterization

For the fabrication of the present (de)multiplexer, the process was started from a 220 nm-thick SOI wafer. An E-beam lithography process with MA-N2403 photoresist was carried out to

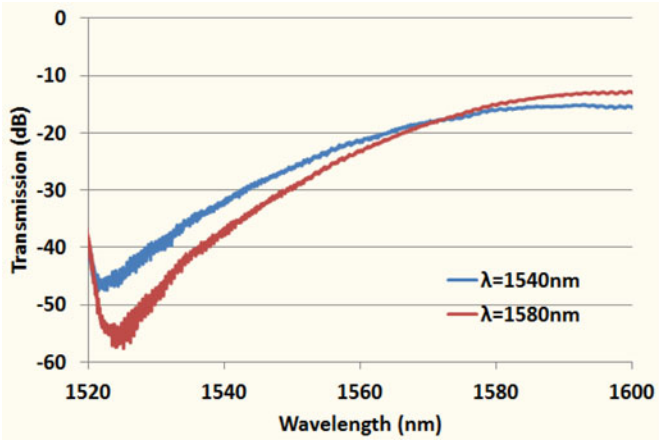

Fig. 4. Measured transmissions for the same straight waveguide when the fiber alignment is optimized for different wavelengths $\lambda = 1540$, and 1580 nm.

make the waveguide pattern, which is then transferred to the silicon layer with an inductively coupled plasma (ICP) etching process. Grating couplers are then made with another shallow-etching process to achieve efficient coupling between the fibers and the chip. Finally PMMA photoresist is spin-coated on top of the devices to form a thin file for protection.

For the characterization of photonic integrated devices, a popular method is using the setup with a tunable laser and a power-meter. In this case, the positions of the input/output fibers are aligned carefully to have a maximal transmission for a given wavelength λ_0. On the other hand, it is well known that the coupling efficiency of a grating coupler is wavelength-sensitive and the central wavelength with the maximal coupling efficiency is dependent on the longitudinal position of the fiber. When one chooses different laser wavelength λ_0 for the fiber alignment, the fiber will be aligned to the different longitudinal position of the grating coupler and thus one obtains different spectral responses for the same straight waveguide with grating couplers (see Fig. 4). Therefore, one should choose the same laser wavelength for the fiber alignment when characterizing the devices, which is feasible for measuring straight waveguides with grating couplers because of the broadband spectral response. However, when measuring the spectral responses of an AWG, one can not choose the same laser wavelength for the fiber alignment to measure all the *N* channels because of the wavelength selectivity of the AWG. Instead, the fiber is usually aligned optimally for the corresponding central wavelength of any AWG channel to be measured. Accordingly, in order to make the normalization for the transmission responses of the *N* channels of AWG, the reference straight waveguide should also be measured *N* times by choosing different laser wavelengths for the fiber alignment, which makes the measurement very inconvenient.

In order to overcome this problem, here the devices were measured by using another setup with a broad-band ASE (amplified spontaneous emission) light source and an optical spectrum analyzer. In this measurement, the fiber alignment is optimized by maximizing the total power in a given wavelength band, e.g., ranging from 1535 to 1565 nm, which corresponds to the wavelength band of our AWG. This rule is complied when

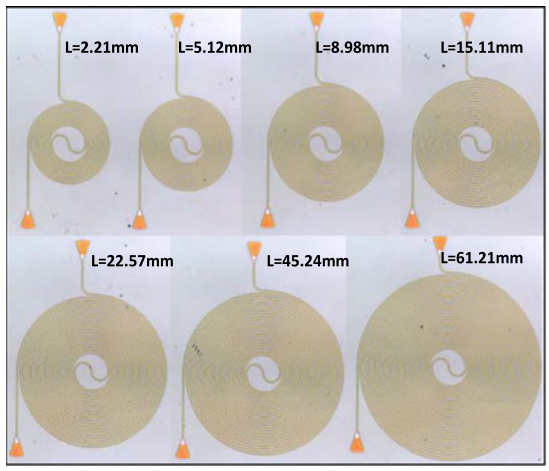

(a)

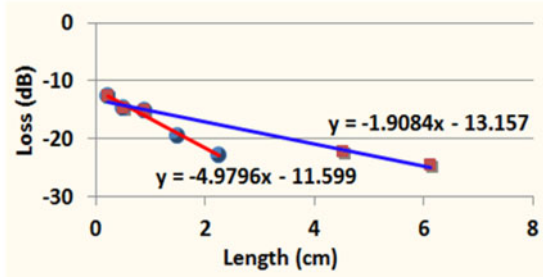

(b)

Fig. 5. SOI nanowire-waveguide spirals. (a) Microscopic images. (b) The measured total loss of these spirals (consisting of the fiber-chip coupling loss).

measuring the devices (e.g., AWGs, and MZIs) as well as the straight waveguides so that the measurement results can be normalized conveniently.

Fig. 5(a) shows the fabricated spiral structures with different lengths, which are designed to estimate the propagation loss of our fabricated SOI nanowire waveguides. Here the cross section of the SOI nanowires is chosen to be 460 nm $\times$ 220 nm to meet the single mode condition. For the spirals, the minimal bending radius for the S-bend in the middle is 15 μm, which is large enough to guarantee a negligibly low bending loss [32]. Therefore, the total propagation loss is assumed reasonably to be proportional to the length of the spiral. For the present case, the length for the longest spiral waveguide is up to 6.1 cm so that the total propagation loss is measurable regarding the propagation loss per unit length is small, which helps to extract the propagation loss per unit length. The measured total losses of all these spirals for the fundamental TE mode are shown in Fig. 5(b). From this figure, the propagation loss of the fabricated SOI nanowires is estimated to be 1.9 $\sim$ 5 dB/cm, which is reasonable and acceptable in comparison with the reported values in the literatures [33], [34].

Fig. 6 shows the optical micrographs for the fabricated device. The footprint of the present wavelength division (de)multiplexer is 520 μm $\times$ 190 μm (not including the expanded output waveguides), which is $\sim$50% smaller than the design with two AWGs shown in Fig. 1. Fig. 7 shows the measured transmission responses of an MZI-based optical interleaver on the same chip.

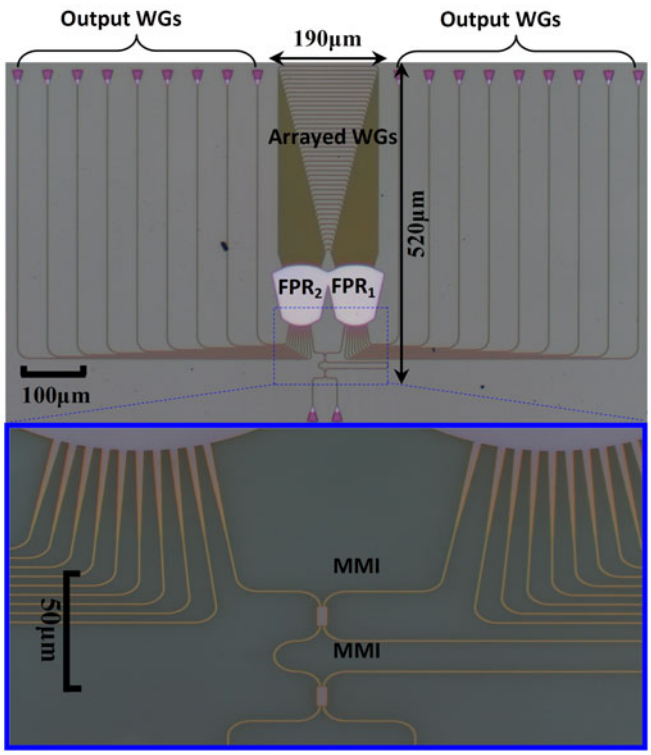

Fig. 6. Microscopic images of the fabricated bi-directional AWG and MZI based interleaver.

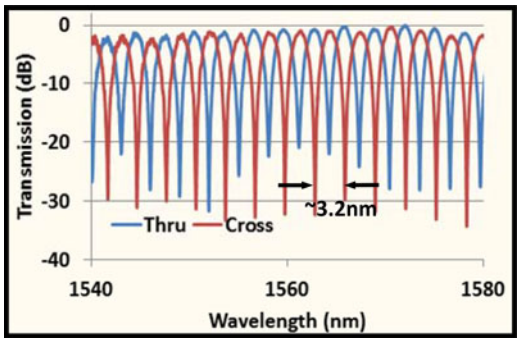

Fig. 7. Measured transmission of the fabricated MZI-based optical interleaver with 2 × 2 MMI couplers.

From this measurement result, it can be seen that the FSR of the MZI is about 3.2 nm, which is consistent with the design value. The excess loss is estimated to be ∼1.0 dB around the central wavelength 1550 nm. It is also observed that the extinction ratio at the cross port is over 30 dB in a wide wavelength range. This is because that the extinction of the cross port is high intrinsically in theory [35]. In contrast, the extinction ratio for the through port is dependent on the wavelength dependence of the power splitting ratio of the MMI coupler. The un-balance of the MMI-based 3 dB coupler degrades the extinction at the through port.

Fig. 8(a) shows the measured spectral responses for all the 18 channels of the present dense wavelength division (de)multiplexer comprising an MZI interleaver and a

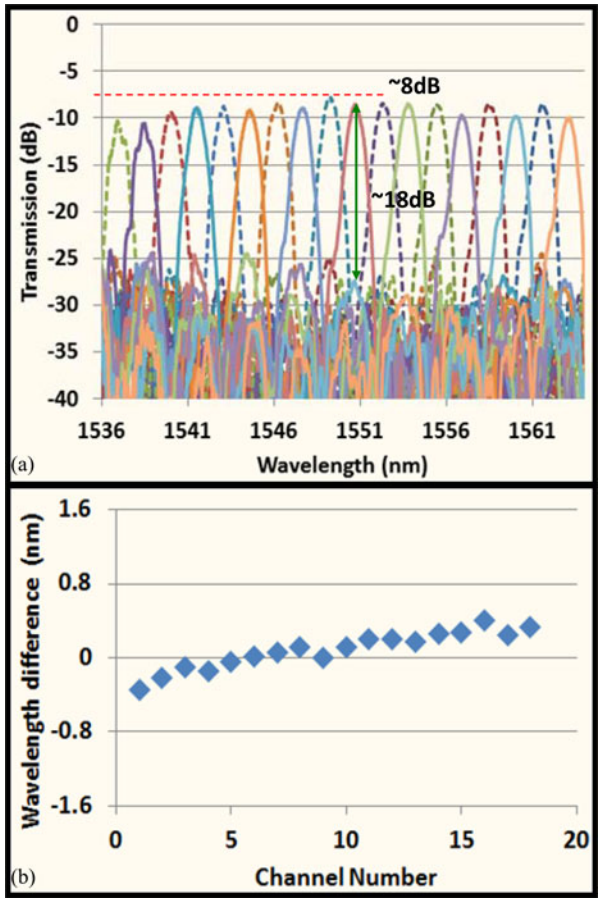

Fig. 8. Measured results of the fabricated 18-channel de-multiplexer with a channel spacing of 200 GHz. (a) The measured spectral responses for all the channels. Dashed lines are for the odd channels, while the solid lines are for the even channels. (b) The wavelength difference between the MZI-based interleaver and the bi-directional AWG for all the wavelength channels.

bi-directional AWG. The solid curves are for the odd channels from the ports at the right side, while the dashed curves are for the even channels from the ports at the left side. It can be seen that these two groups of channels are interleaved very well with a wavelength offset of 1.6 nm. This is guaranteed intrinsically by such a bi-directional AWG working as two AWGs sharing the identical dispersion AWG. The excess loss for the central channel is about 8 dB, which mainly from the MZI as well as the AWG. According to our measurement results for them separately, the MZI interleaver and the bi-directional AWG contribute an excess loss of ∼2 and ∼6 dB, respectively. Particularly, for the bi-directional AWG, there is an extra loss due to the input waveguide positioned at the edge and this extra loss is estimated to be ∼1.5 dB according to the formula given in [36]. From Fig. 8(a), it can be seen that the channel non-uniformity is about 2 dB, which is partially from the intrinsic channel non-uniformity of an AWG according to [36]. The MZI-based optical interleaver also introduces some non-uniformity due to the wavelength misalignment between the MZI and the AWG. The channel crosstalk is about $-15 \sim -18$ dB, which is similar to a compact nine-channel AWG with a channel spacing of 3.2 nm fabricated on the same chip.

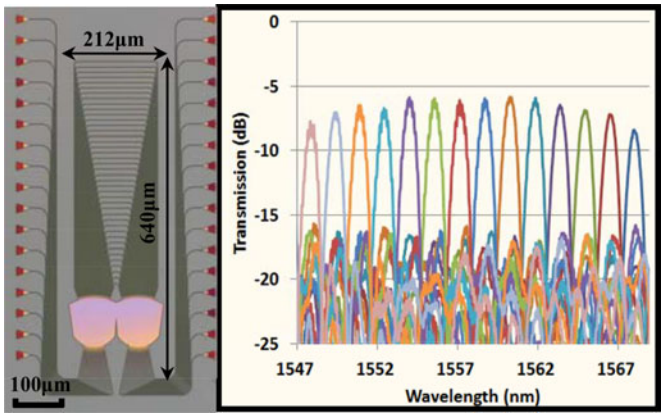

Fig. 9. Measured spectral responses for the fabricated simple regular AWG with a channel spacing of 200 GHz.

TABLE I
COMPARISON BETWEEN A SIMPLE REGULAR 200 GHZ AWG AND THE PRESENT (DE)MULTIPLEXER

	Simple regular AWG	The present device
Channel spacing (GHz)	200	200
Device footprint (μm $\times$ μm)	640 $\times$ 212	520 $\times$ 190
Channel Number	14	18
Crosstalk (dB)	~ -10	~ -18
Excess loss (dB)	$\sim$6	$\sim$8

Besides, we make a comparison for all the wavelength channels of the fabricated de-multiplexer (including a MZI and a bi-directional AWG), with that of a single MZI fabricated on the same chip, as shown in Fig. 8(b). The deviation is less than 0.5 nm, which is due to the mismatch between the MZI's FSR and the AWG's channel spacing, resulting from the fabrication errors. This acceptable value for the wavelength misalignment is attributed to the excellent E-beam lithography and ICP etching processes. It is possible to further improve the wavelength alignment when the responses of the AWG and the MZI are flattened by introducing special designs [19], [37].

In order to give a comparison, we also fabricated a simple regular 14-channel AWG with a channel spacing of 200 GHz (see the inset in Fig. 9) and the measured spectral responses are shown in Fig. 9. Table I gives a comprehensive comparison between the simple regular AWG and the present (de)multiplexer. It can be seen that the device footprint is shrunk by 27% with the present design in comparison with the simple regular AWG. Furthermore, the present (de)multiplexer has much lower channel crosstalk (~ -18 dB) than the regular 200 GHz AWG (whose crosstalk is about -10 dB). On the other hand, the excess loss for the present (de)multiplexer becomes higher in some degree due to the introduction of the MZI and the edge input, as predicted.

IV. CONCLUSION

In summary, we have proposed and demonstrated a compact dense wavelength division (de)multiplexer consisting of an asymmetrical MZI-based optical interleaver and a single bi-directional AWG. In this way, the channel number becomes doubled, and the channel spacing becomes halved in comparison with the single AWG. More importantly, the device's footprint only has a slight increase and the performance does not degrade notably. As an example, a 18-channel wavelength division (de)multiplexer with a channel spacing of 200 GHz (i.e., $\Delta\lambda_{\rm ch} = 1.6$ nm) has been realized by using a 10 $\times$ 10 bi-directional AWG with a channel spacing of 400 GHz (i.e., $\Delta\lambda'_{\rm ch} = 3.2$ nm). The device has a footprint of 520 μm $\times$ 190 μm, which is $\sim$50% smaller than the design with two AWGs. According to the measurement results for the fabricated 18-channel 200 GHz (de)multiplexer, it can be seen that the channel crosstalk is $-15 \sim -18$ dB (similar to a single nine-channel 400 GHz AWG on the same chip). The excess loss increases by 2 dB due to the cascaded MZI optical interleaver.

REFERENCES

[1] D. Dai and J. E. Bowers, "Silicon-based on-chip multiplexing technologies and devices for Peta-bit optical interconnects," *Nanophotonics*, vol. 3, pp. 283–311, 2014.
[2] S. Xiao, M. H. Khan, H. Shen, and M. Qi, "Multiple-channel silicon micro-resonator based filters for WDM applications filters for WDM applications," *Opt. Exp.*, vol. 15, pp. 7489–7498, 2007.
[3] M. S. Dahlem, C. W. Holzwarth, A. Khilo, F. X. Kärtner, H. I. Smith, and E. P. Ippen, "Reconfigurable multi-channel second-order silicon microring-resonator filterbanks for on-chip WDM systems," *Opt. Exp.*, vol. 19, pp. 306–316, 2011.
[4] S. Park, K. Kim, I. Kim, and G. Kim, "Si micro-ring MUX/DeMUX WDM filters," *Opt. Exp.*, vol. 19, pp. 13531–13539, 2011.
[5] P. D. Heyn, J. D. Coster, P. Verheyen, G. Lepgae, M. Pantouvaki, P. Absil, W. Bogaerts, J. V. Campenhout, and D. V. Thourhout, "Fabrication-tolerant four-channel wavelength division multiplexing filter based on collectively tuned Si microrings," *J. Lightw. Technol.*, vol. 31, no. 16, pp. 2785–2792, Aug. 2013.
[6] P. Chen, S. Chen, X. Guan, Y. Shi, and D. Dai, "High-order microring resonators with bent couplers for a box-like filter response," *Opt. Lett.*, vol. 39, pp. 6304–6307, 2014.
[7] J. Brouckaert, W. Bogaerts, P. Dumon, D. V. Thourhout, and R. Baets, "Planar concave grating demultiplexer fabricated on a nanophotonic silicon-on-insulator platform," *J. Lightw. Technol.*, vol. 25, no. 5, pp. 1269–1275, May 2007.
[8] B. B. C. Kyotoku, L. Chen, and M. Lipson, "Broad band 1 nm channel spacing silicon-on-insulator wavelength division multiplexer," in *Proc. IEEE Conf. Laser Electro-Optics*, 2009, pp. 1–2.
[9] R. Adar, C. Henry, C. Dragone, R. Kistler, and M. Milbrodt, "Broad-band array multiplexers made with silica waveguides on silicon," *J. Lightw. Technol.*, vol. 11, no. 2, pp. 212–219, Feb. 1993.
[10] M. Zirngibl, C. Dragone, and C. Joyner, "Demonstration of a 15$\times$15 arrayed waveguide multiplexer on InP," *IEEE Photon. Technol. Lett.*, vol. 4, no. 11, pp. 1250–1253, Nov. 1992.
[11] B. Yang, Y. Zhu, Y. Jiao, L. Yang, Z. Sheng, S. He, and D. Dai, "Compact arrayed waveguide grating devices based on small SU-8 strip waveguides," *J. Lightw. Technol.*, vol. 29, no. 13, pp. 2009–2014, Jul. 2011.
[12] D. Dai, Z. Wang, J. F. Bauters, M. C. Tien, M. J. R. Heck, D. J. Blumenthal, and J. E. Bowers, "Low-loss Si_3N_4 arrayed-waveguide grating (de)multiplexer using nano-core optical waveguides," *Opt. Exp.*, vol. 19, pp. 14130–14136, 2011.
[13] L. Chen, C. R. Doerr, L. Buhl, Y. Baeyens, and R. A. Aroca, "Monolithically integrated 40-wavelength demultiplexer and photodetector array on silicon," *IEEE Photon. Technol. Lett.*, vol. 23, no. 13, pp. 869–871, Jul. 2011.
[14] D. Dai, L. Liu, L. Wosinski, and S. He, "Design and fabrication of ultra-small overlapped AWG demultiplexer based on α-Si nanowire waveguides," *Electron. Lett.*, vol. 42, pp. 400–402, 2006.
[15] D. Dai, X. Fu, Y. Shi, and S. He, "Experimental demonstration of an ultracompact Si-nanowire-based reflective arrayed-waveguide grating (de)multiplexer with photonic crystal reflectors," *Opt. Lett.*, vol. 35, pp. 2594–2596, 2010.

[16] S. Pathak, D. Van Thourhout, and W. Bogaerts, "Design trade-offs for silicon-on-insulator-based AWGs for (de)multiplexer applications," *Opt. Lett.*, vol. 38, pp. 2961–2964, 2013.
[17] K. Okamoto and K. Ishida, "Fabrication of silicon reflection-type arrayed-waveguide gratings with distributed Bragg reflectors," *Opt. Lett.*, vol. 38, pp. 3530–3533, 2013.
[18] J. Wang, Z. Sheng, L. Li, A. Pang, A. Wu, W. Li, X. Wang, S. Zou, M. Qi, and F. Gan, "Low-loss and low-crosstalk 8 × 8 silicon nanowire AWG routers fabricated with CMOS technology," *Opt. Exp.*, vol. 22, pp. 9395–9403, 2014.
[19] S. Pathak, M. Vanslembrouck, P. Dumon, D. V. Thourhout, and W. Bogaerts, "Optimized silicon AWG with flattened spectral response using an MMI aperture," *J. Lightw. Technol.*, vol. 31, no. 1, pp. 87–93, Jan. 2013.
[20] P. Cheben, J. H. Schmid, A. Delage, A. Densmore, S. Janz, B. Lamontagne, J. Lapointe, E. Post, P. Waldron, and D. Xu, "A high-resolution silicon-on-insulator arrayed waveguide grating microspectrometer with submicrometer aperture waveguides," *Opt. Exp.*, vol. 15, pp. 2299–2306, 2007.
[21] S. Cheung, T. Su, K. Okamoto, and S. J. B. Yoo, "Ultra-compact silicon photonic 512×512 25 GHz arrayed waveguide grating router," *IEEE J. Sel. Topics Quantum Electron.*, vol. 20, no. 4, pp. 310–316, Jul./Aug. 2014.
[22] L. Xiang, Y. Yu, D. Gao, M. Ye, B. Zou, and X. Zhang, "Silicon based integrated comb filter and demultiplexer for simultaneous WDM signal processing," *IEEE J. Sel. Topics Quantum Electron.*, vol. 20, no. 4, pp. 240–247, Jul./Aug. 2014.
[23] L. Zhou, T. Ye, and J. Chen, "Coherent interference induced transparency in self-coupled optical waveguide-based resonators," *Opt. Lett.*, vol. 36, pp. 13–15, 2011.
[24] Y. Hu, X. Xiao, H. Xu, X. Li, K. Xiong, Z. Li, T. Chu, Y. Yu, and J. Yu, "High-speed silicon modulator based on cascaded microring resonators," *Opt. Exp.*, vol. 20, pp. 15079–15085, 2012.
[25] H. Yi, D. S. Citrin, Y. Chen, and Z. Zhou, "Dual-microring-resonator interference sensor," *Appl. Phys. Lett.*, vol. 95, p. 191112, 2009.
[26] M. Abe, Y. Hibino, T. Tanaka, M. Itoh, A. Himeno, and Y. Ohmori, "Mach-Zehnder interferometer and arrayed-waveguide-grating integrated multi/demultiplexer with photosensitive wavelength tuning," *Electron. Lett.*, vol. 37, pp. 376–377, 2001.
[27] W. Bogaerts, D. Taillaert, P. Dumon, D. V. Thourhout, and R. Baets, "A polarization-diversity wavelength duplexer circuit in silicon-on-insulator photonic wires," *Opt. Exp.*, vol. 15, pp. 1567–1578, 2007.
[28] L. Chen, C. R. Doerr, and Y. Chen, "Polarization-diversified DWDM receiver on silicon free of polarization-dependent wavelength shift," presented at the Optical Fiber Communication Conf., Los Angeles, CA, USA, 2012, p. OW3G. 7.
[29] D. Keil and E. Anderson, "Characterization of reactive ion etch lag scaling," *J. Vac. Sci. Technol. B*, vol. 19, pp. 2082–2088, 2001.
[30] Y. Shi, S. He, and S. Anand, "Ultracompact directional couplers realized in InP by utilizing feature size dependent etching," *Opt. Lett.*, vol. 33, pp. 1927–1929, 2008.
[31] A. V. Velasco, M. L. Calvo, P. Cheben, P. A. Ortega-Monux, J. H. Schmid, C. A. Ramos, I. M. Fernandez, J. Lapointe, M. Vachon, S. Janz, and D. Xu, "Ultracompact polarization converter with a dual subwavelength trench built in a silicon-on-insulator waveguide," *Opt. Lett.*, vol. 37, pp. 365–367, 2012.
[32] D. Dai, Y. Shi, and S. He, "Characteristic analysis of nanosilicon rectangular waveguides for planar light-wave circuits of high integration," *Appl. Opt.*, vol. 45, pp. 4941–4946, 2006.
[33] W. Bogaerts, P. Dumon, D. Thourhout, D. Tailaert, P. Jaenen, J. Wouters, S. Beckx, V. Wiauz, and R. Baets, "Compact wavelength-selective functions in silicon-on-insulator photonic wires," *IEEE J. Sel. Topics Quantum Electron.*, vol. 12, no. 6, pp. 1394–1401, Nov./Dec. 2006.
[34] T. Tsuchizawa, K. Yamada, H. Fukuda, T. Watanabe, S. Uchiyama, and S. Itabashi, "Low-loss Si wire waveguides and their application to thermooptic switches," *Jpn. J. Appl. Phys.*, vol. 45, pp. 6658–6662, 2006.
[35] D. Dai, Z. Wang, and J. E. Bowers, "Considerations for the design of asymmetrical Mach-Zehnder interferometers used as polarization beam splitters on a sub-micron silicon-on-insulator platform," *J. Lightw. Technol.*, vol. 29, no. 12, pp. 1808–1817, Jun. 2011.
[36] M. K. Smit and C. V. Dam, "PHASAR-based WDM-devices: Principles, design and applications," *IEEE J. Sel. Topics Quantum Electron.*, vol. 2, no. 2, pp. 236–250, Jun. 1996.
[37] J. Song, Q. Fang, S. H. Tao, M. B. Yu, G. Q. Lo, and D. L. Kwong, "Passive ring-assisted Mach-Zehnder interleaver on silicon-on-insulator," *Opt. Exp.*, vol. 16, pp. 8359–8365, 2008.

Sitao Chen received the B.Eng. degree from the Department of Optical Engineering, Zhejiang University, Hangzhou, China, in 2011, where he is currently working toward the Ph.D. degree in the same department. His research interests include silicon wavelength-division (de)multiplexers.

Xin Fu received the B.Eng. degree from the Department of Optical Engineering, Zhejiang University, Hangzhou, China, in 2010, where she is currently working toward the Ph.D. degree in the same department. Her research interests include silicon hybrid photonic integrated devices.

Jian Wang received the B.Eng. degree from the Nanjing University of Technology, Nanjing, China, in 2010. He is currently working toward the Ph.D. degree in the Department of Optical Engineering, Zhejiang University, Hangzhou, China. His research interests include on-chip mode (de)multiplexers.

Yaocheng Shi received the B.Eng. degree from Department of Optical Engineering, Zhejiang University, Hangzhou, China, and the Ph.D. degree from the Royal Institute of Technology, Stockholm, Sweden, in 2003 and 2008, respectively. He joined Zhejiang University as an Assistant Professor in 2008 and became an Associate Professor in 2010. His research interests include silicon photonic integrated devices. He has published >40 refereed international journals papers.

Sailing He (M'92–SM'98–F'13) received the Ph.D. degree from the Royal Institute of Technology (KTH), Stockholm, Sweden, in 1992. Since then, he has been at KTH as an Assistant Professor, an Associate Professor, and a Full Professor. Currently, he is also a National Distinguished Professor appointed by China's central government (through Qian-Ren program) and a Chief Scientist for the Joint Research Center of Photonics of KTH, Stockholm, and Zhejiang University, Hangzhou, China. He has authored one monograph (Oxford University Press) and about 500 papers in refereed international journals. His current research interests include metamaterials, biophotonics, photonic integration technologies, fiber optical communication technologies, and optical sensing technologies. He is a Fellow of the OSA, SPIE, and The EM Academy.

Daoxin Dai (M'07) received the B.Eng. degree from the Department of Optical Engineering, Zhejiang University, Hangzhou, China, and the Ph.D. degree from the Royal Institute of Technology (KTH), Stockholm, Sweden, in 2000 and 2005, respectively. Then he joined Zhejiang University as an Assistant Professor and became an Associate Professor in 2007, and a Full Professor in 2011. He worked at the University of California at Santa Barbara as a Visiting Scholar from 2008 until 2011. His research interests include silicon photonic integrated devices and the applications. He has published >120 refereed international journals papers (including seven invited review papers). He is serving as the Associate Editor of the journals of IEEE PHOTONICS TECHNOLOGY LETTERS, *Optical and Quantum Electronics*, and *Photonics Research*.